Long-range suppressive influences from the visual surround can be explained by anatomically plausible recruitment of local competition in a model of columnar cortex

Short title: Surround suppression through local competition

Hongzhi You[1,2], Giacomo Indiveri[1,*], Dylan R. Muir[3,*]

1 Institute of Neuroinformatics, University / ETH Zürich, Zürich, Switzerland
2 Key Laboratory for NeuroInformation of Ministry of Education, Center for Information in BioMedicine, University of Electronic Science and Technology of China, Chengdu, China
3 Biozentrum, University of Basel, Basel, Switzerland

* dylan.muir@unibas.ch, giacomo@ini.uzh.ch

Abstract

Although neurons in columns of tissue in visual cortex of adult carnivores and primates share similar preferences for the orientation of a visual stimulus [1, 2], they can nevertheless have sparse and temporally uncorrelated firing visual response properties [3–5]. This effect is supported by the observation that long-range excitatory connections between cortical neurons are functionally specific, because they interconnect columns with similar orientation preference [6, 7], and local short-range ones are unspecific and sparse. Coupled with strong local inhibition, this network architecture is a good recipe for local competition arranged within a cortical column [8]. In this paper we propose a model architecture that is consistent with these experimental and anatomical findings, and which explains the emergence of orientation-tuned surround suppression. We explore the effect of local columnar competition, coupled with local and long-range functional specificity, as substrates for integration of responses from the visual surround in columnar visual cortex. In addition, we show how presentation of simulated full-field complex visual stimuli, designed to approximate visual scenes, leads to reduced correlation of local excitatory responses and increased excitatory response selectivity (lifetime sparseness). These effects occurred simultaneously with increased inhibitory activity and decreased inhibitory sparseness, consistent with recordings of excitatory and inhibitory neurons in cortex [9, 10]. In our networks competition, reduced correlation and increased sparseness depended on both local and long-range specific excitatory connectivity. The mechanism of local competition implemented in our model explains several aspects of integration of information from the visual surround, and is consistent with experimentally measured spatial profiles of cortical excitation and inhibition.

Author Summary

Cells in the visual areas of the brain are active when an image appears in a small area of visual space. But the way a cell responds also depends on what images cover the rest of visual space, in complex ways that we don't yet understand. In experiments, this leads to some cells shutting down when visual patterns are shown to an animal on a screen. We developed a computational model for the visual processing areas of the brain, in animals such as cats, monkeys and humans

that explains this phenomenon: we propose that nearby nerve cells in the brain compete with each other when they respond to visual information coming from the eye. In our model, this competition leads to some nerve cells shutting down, in a similar way as is seen in experiments with real brains. Ensuring that only a few nerve cells are active makes the brain more efficient at responding to the visual world. This is a general principle that could very well be in place also in other areas of the brain. We believe that this model will lead to a better understanding of how networks of nerve cells in the brain are connected and share information.

Introduction

In species with highly developed neocortices, such as cats and primates, cortical neurons are grouped into columns that share functional similarities [11]. In primary visual cortex, columns of neurons have highly similar preferred orientations of a visual stimulus [1, 2]. However, given that neurons in a column share the same retinotopic location and a common orientation preference, the firing activity of these neurons is surprisingly poorly correlated [3, 4, 12], even in response to drifting grating stimuli [3, 12].

As natural sensory inputs are highly temporally correlated [13, 14], an active mechanism to reduce correlations is required to improve information coding efficiency [14, 15]. This is because strong correlations across a population can impair the ability to extract information from a population responding to a sensory stimulus [16, 17]. "Sparse coding" of responses to sensory stimuli is a valuable goal for cortex, which serves to increase the storage capacity [18, 19] and information efficiency [16, 17] of cortical populations. In visual cortex, the functional relationships between nearby neurons is modulated by the influence of information from the visual surround. Wide-field stimulation with natural scenes promotes more selective and less correlated excitatory activity [9, 10], while inhibitory activity becomes stronger and less selective [10].

How does this reduction in response correlation come about, given the prevalence of strong spatial and temporal correlations present in natural visual scenes [13, 14], and given that neurons in a column share common preferences for visual features? Several neural models have been proposed to reduce correlations in network activity, including nonlinearity of spike generation, synaptic-transmission variability and failure, short-term synaptic depression, heterogeneity in network connectivity, intrinsic neuronal properties and recurrent network dynamics [20–24]. A particularly appealing form of recurrent dynamics is that involving inhibitory feedback loops, which are abundant in cortical networks [12, 14, 15, 24–27]. When configured appropriately, inhibitory feedback promotes competition between the activity of a set of excitatory neurons, such that weaker responses are suppressed in a non-linear fashion [28–31].

Local excitatory connections are sparse in cortex, with maximum connection probabilities between closest proximal cells (i.e. $\approx 50\,\mu m$) of only 20 % to 30 % [32–35] and with connection probability falling off sharply with distance [36, 37]. In contrast, local connections between excitatory and inhibitory neurons are dense in rodents [38–41]. In animals with columnar visual cortices, inhibitory inputs are simply integrated from the nearby surrounding tissue [42], suggesting a similar pattern of dense local connectivity. Long-range excitatory connections (i.e. $500\,\mu m$ to $1500\,\mu m$) within columnar visual cortex are made selectively between points across the cortical surface with similar functional preferences [6, 7, 43–47]. Similarly, excitatory connections in rodents are made selectively [32, 48], between neurons with correlated functional properties [34, 41, 49].

We propose a novel competitive model that exploits excitatory interaction between long-range and local cortical circuits connecting neurons in the superficial layers of cortex. These excitatory interactions produce locally-mediated competition within a cortical column,

which can be recruited or modulated by information conveyed over long-range excitatory projections, including from the visual surround. As discussed above, competition directly reduces correlations within a network (in the sense of making correlation coefficients more negative); however, if competition were to occur within a cortical column, a few "winning" neurons would increase their activity, while that majority of "losing" neurons would decrease their activity. We therefore propose that the physiology of "losing" neurons is highly similar to suppression of neural responses provoked by surround stimulation.

Grating stimuli presented in the visual surround predominately suppress neural responses [50–57], with more than 50% of neurons reducing their firing rate [53]. The degree of suppression is sensitive to the grating stimulus orientation presented within the classical receptive field (cRF) and visual surround, with strongest suppression occurring when the orientations within the cRF and surround match [51, 53, 55]. Surprisingly, the tuning of peak suppression is not determined by the preferred orientation of the neuron being suppressed. Instead, peak suppression occurs when cRF and surround orientations are aligned, regardless of the preferred orientation of the neuron being recorded [57]. Indeed, the expression of surround suppression depends on the local structure of the orientation map in V1 [58]. Consistent with a local competitive mechanism, a comparatively smaller proportion of neurons undergo facilitation in response to surround stimulation [52, 53, 59].

Here we investigate the ability of a local competitive mechanism, operating within a cortical column, to explain features of visual responses provoked by stimulation in the visual surround. We design a model for the superficial layers of cat primary visual cortex (area 17), including several populations designed to simulate distinct portions of the visual field ("centre" and "surround"). We present several simulated visual stimuli, designed in analogy to experimental investigations of centre/surround visual interactions, and show how the mechanism of local competition is recruited by visual stimulation to reduce local correlations and to suppress neuronal responses.

Results

Network architecture

We developed a spiking network model for adult columnar primary visual cortex, composed of 7 populations of neurons, each representing a distinct location on the visual field (Fig. 1a; see Methods). Each population consisted of a ring representing one hypercolumn — a full ordered sequence of preferred orientations corresponding to approximately 1 mm of cat area 17 [47]. One population was arbitrarily chosen as the *center* of visual stimulation; the other populations represented *surround*ing areas of visual space (i.e. the visual surround). Each population was composed of a series of columns consisting of excitatory and inhibitory neurons, where each column contained neurons with a common preferred orientation. Inhibitory neurons made only short-range recurrent connections within their source population; in contrast, excitatory neurons made wider-ranging recurrent connections within their source population, as well as long-range connections to the other populations in the model (Fig. 1b). All connections were made symmetrically following Gaussian profiles over difference in preferred orientation, taking into account the ring topology within each population. Long-range connections were therefore biased to connect columns with similar orientation preference, as is observed in cat visual cortex [7, 47]. In this paper, we refer to this form of functional synaptic specificity as θ-*specific* (i.e. orientation-specific).

Within each column, excitatory neurons were assumed to form sub-populations ("specific subnetworks", or SSNs; Fig. 1c), which have a higher-than-chance probability of forming
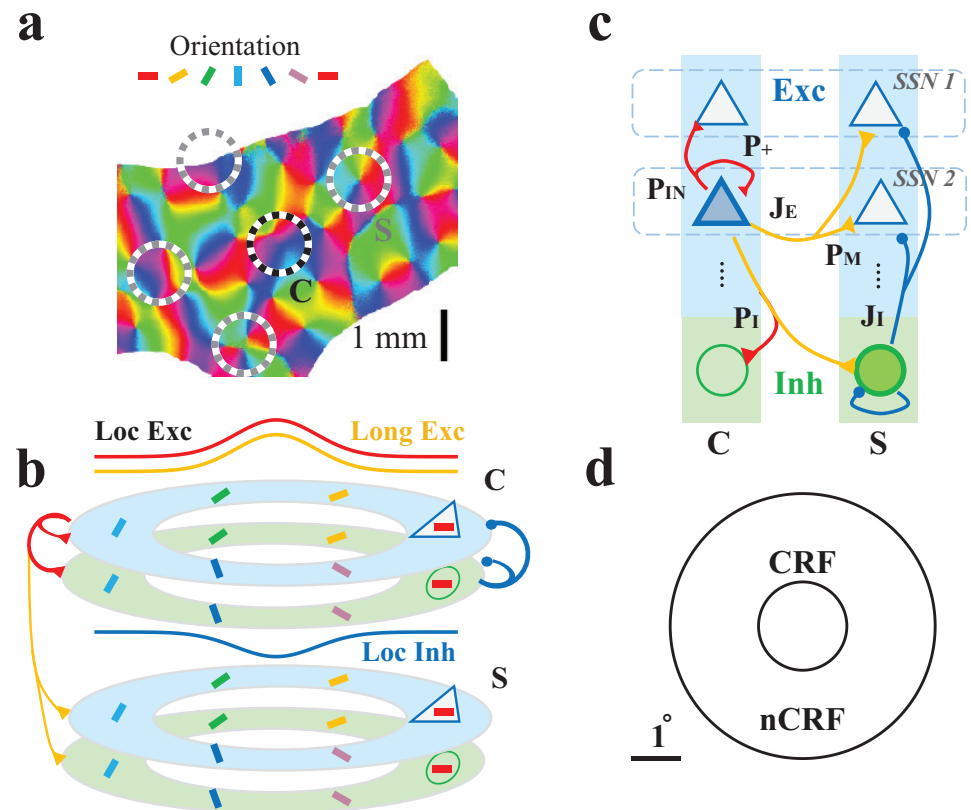
Figure 1. The network architecture of the center-surround model. (a) We simulated several populations representing non-overlapping locations in primary visual cortex (dashed cicrles), covering distinct locations of the visual field. Each population was simulated as a ring of neurons considered to span an orientation hypercolumn, i.e. containing a set of columns with a complete ordered sequence of orientation preferences. One population ("C") corresponded to the centre of visual stimulation; the others corresponded to the visual surround ("S"). (b) Excitatory (triangles) and inhibitory neurons (circles) in each population were arranged in orientation columns around the ring, with preferred orientations indicated by coloured bars. Local excitatory and inhibitory connections within each population, as well as long-range excitatory connections between populations, were modelled as Gaussian fields over difference in preferred orientation (curves in b). For simplicity only projections from a single population are shown ("C" ring; upper); connections were made identically within and between each population in the model. (c) Connections from single neurons were made both within a column, and between populations. Excitatory neurons within a column were distributed evenly across several subnetworks (SSNs; see Methods for details of parameters). A proportion of local excitatory synapses was reserved to be made only with other neurons within the same SSN (P_+). Long-range excitatory connections were also sensitive to SSN membership, under the parameter P_M. J_E, J_I: Strength of excitatory (E) and inhibitory (I) synapses. P_{IN}, P_I: Fraction of synapses onto excitatory (IN) and inhibitory (I) targets made locally within the same hypercolumn, as opposed to long-range projections to other hypercolumns. For simplicity, only connections from a single excitatory and inhibitory neuron are shown; projection rules are identical for all neurons in the model. (d) Placed in visual space, the central population corresponded to approximately 1° of visual space; the surround populations were defined to cover approximately 4.5° of visual space.

recurrent excitatory connections. In contrast, inhibitory neurons have equal probabilities of forming recurrent inhibitory connections to all neurons within a column, regardless of SSN

membership. This architecture is known to exist in rodent visual cortex [32, 34, 41, 48, 49], but has not been examined experimentally or computationally in columnar visual cortex. In this paper we refer to this form of specificity as *SSN-specific* connectivity. SSN-specificity in our model could be replaced by the presence of strong recurrent excitatory feedback on the scale of single cortical neurons, if necessary. The strength of SSN-specificity was under the control of a parameter P_+ (see Methods). As $P_+ \to 1$, all excitatory connections are made within the same SSN. As $P_+ \to 1/M$, all synapses are distributed equally across all SSNs; equivalent to fully random connectivity within a column (here, M is the number of SSNs in each column). Long-range connections were also SSN-specific under the control of a parameter P_M (with analogous definition as P_+). All parameter values were selected to be realistic estimates for cat area 17 (see Table 1).

Our model examined modulation of orientation-tuned responses, caused by inputs from the visual surround, carried by long-range excitatory connections within the superficial layers of columnar cortex. Our model did not investigate the emergence of orientation tuning, which occurs from convergence of thalamic afferents into cortex [60]. We assumed that the neurons in our model resided in the superficial layers of cortex, and therefore received orientation-tuned input primarily from layer 4.

Neurons within a column are similarly tuned, but without temporally correlated responses

We tested the response of our model to simulated grating visual stimuli, presented first to the classical receptive field only (cRF; centre-only stimulus), and under wide-field stimulation (centre-surround stimulus) (Fig. 2). Stimulation of the cRF with grating stimuli of a single orientation provoked a response over the central population according to the similarity between the stimulus and the preferred orientation of each column (Fig. 2a).

Orientation tuning curves were similar between excitatory and inhibitory neurons (Fig. 2e; tuning widths 25.9° half-width at half-height for excitatory neurons and 27.1° for inhibitory neurons; $P < 10^{-10}$, t-test, 200 neurons). Although neurons within the same column were tuned to identical preferred orientations and responded with a higher average firing rate to the same stimuli, temporal patterns of activation were weakly but significantly negatively correlated on average within a column (Fig. 2c and f; median corr. -0.06; $P < 10^{-10}$, rank-sum test, 200 trials).

Wide-field presentation of simulated grating stimuli provoked stronger negative correlations between neurons within a column (Fig. 2b, d and f; median corr. -0.06 vs -0.24; $P < 10^{-10}$, rank-sum test, 200 trials). Wide-field stimulation also increased the firing rate of the inhibitory population (21.2 Hz to 26.0 Hz; $P < 10^{-10}$, t-test, 200 trials) and decreased the firing rate of the excitatory population (16.4 Hz to 11.7 Hz; $P < 10^{-10}$, t-test, 200 trials), consistent with experimental observations in visual cortex [10]. The orientation tuning width of inhibitory neurons increased slightly under wide-field stimulation (27.1° to 28.0°; $P < 10^{-10}$, t-test, 200 trials).

Non-random excitatory connectivity promotes negative correlation of neural responses

What parameters of cortical connectivity lead to competition in response to centre-surround stimulation? We explored the dependence of competition on the degree of non-random connectivity, both local (P_+) and long-range projections (P_M; see Methods). We simulated the presentation of wide-field stimulation with grating stimuli, as in Fig. 2, and measured the
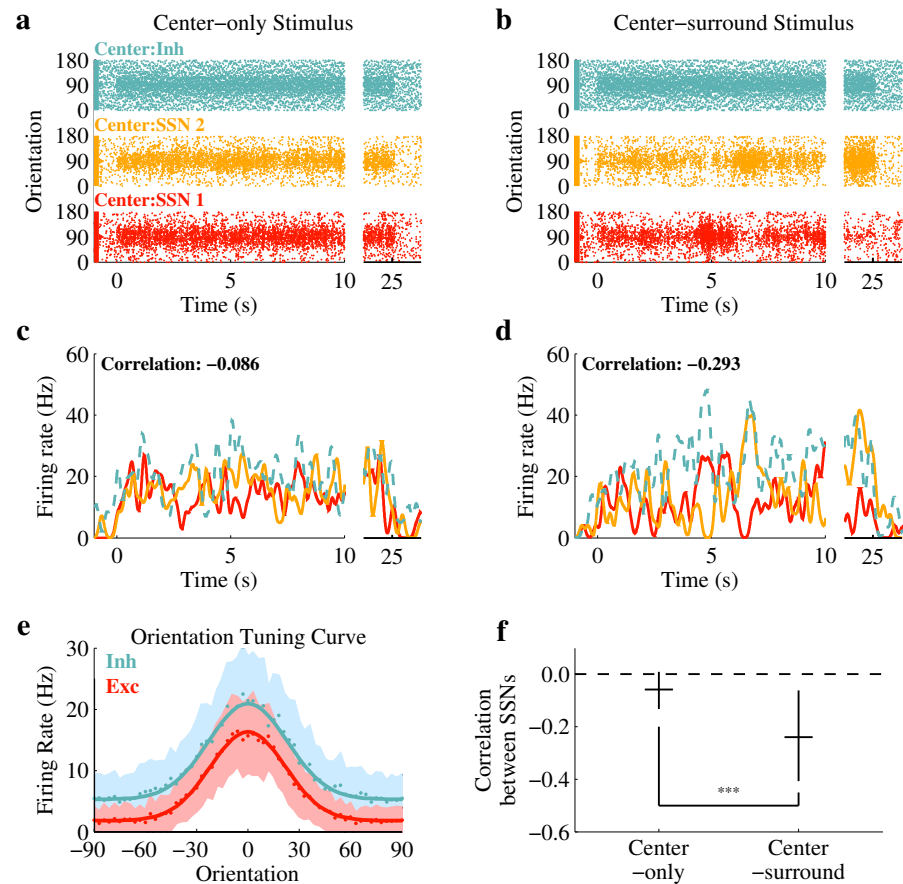
Figure 2. Neurons within a column are not temporally correlated in response to centre-surround grating stimulation. (a–b) Spiking responses of neurons in the centre population, in response to centre-only (a) and centre-surround stimulation (b) with 90° orientation stimulus. Inhibitory neurons: blue-green; two of four excitatory SSNs: red and yellow. **(c–d)** Firing rates over time for neurons with 90° orientation preference (colours as in a–b). **e** Orientation tuning curves for excitatory and inhibitory neurons are similar. Under centre-only stimulation (a and c), excitatory neurons within a column respond together, since they share a common preferred orientation, but are temporally decorrelated (correlation coefficient close to zero; c and **f**). Under wide-field stimulation (b and d), responses of neurons within the same column become more negatively correlated (negative correlation coefficient; d and f). *** $p < 0.001$.

average correlation coefficient between neurons in the same column. Measurements of correlation coefficients over many network instances with varying P_+ and P_M are shown in Fig. 3. In all cases, connections within and between populations were θ-specific. However, competition depended strongly on non-random excitatory connectivity, such that when connections were made without local or long-range SSN-specificity (i.e. low P_+ and P_M), responses within a column were correlated. In contrast, when connections were highly non-random (i.e. P_+, $P_M \rightarrow 1$) then responses within a column were negatively correlated.

The effects of local and long-range non-random connectivity are mutually supportive. When either of local or long-range connections are made SSN-specific then weak competition is
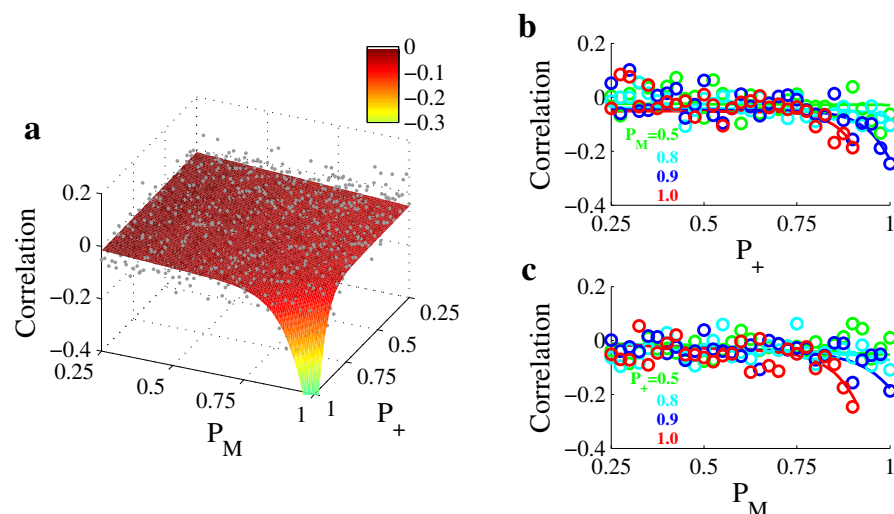
Figure 3. Non-random excitatory connectivity underlies competition and reduced correlation in response to centre-surround stimulation. (a–c) Correlation between the neurons in a column, as a function of the SSN-specificity parameters P_+ and P_M (see Methods; Fig. 1). Grey dots and circles: measurements from individual simulations of the spiking network model. Surface in (a) and curves in (b–c): smooth fit to individual simulations. Both local recurrent specificity (P_+) and long-range specificity (P_M) promote competition within single columns (negative correlation coefficients).

introduced. However, when both connection pathways are SSN-specific then competition is significantly strengthened.

We hypothesised that the negative correlations introduced by non-random connectivity depends on the mechanism of competition within a cortical column. We therefore used nonlinear dynamical analysis to explore the presence of competition within a mean-field version of the model, and the dependence of competition on network parameters. Our mean-field model included only two populations from the full spiking model, with each population reduced to a single column; that is, the orientation-selective profile of connectivity is neglected (see details in **Methods**). In this analysis we systematically vary the parameters of the model under centre-only and centre-surround stimulation, and characterise the strength of competition within a column (Competition Index — CI; see Methods).

Results of this analysis are shown in Fig. 4. In general, increasing the strength of excitatory connections (J_E) increased the strength of competition, and the opposite was true for the strength of inhibitory connections (J_I). Although competition is mediated via disynaptic inhibitory interactions between excitatory neurons, competition also requires strong excitatory interaction within SSNs, and increasing the strength of inhibition reduces the ability of excitatory neurons to recruit others within the same SSN.

Under our estimates for synaptic strengths approximating cortical connectivity (red crosses in Fig. 4a and b; Table 1; see Methods), activity within a column is balanced. Neurons within a column undergo mutual soft winner-take-all competitive interactions (sWTA; gray shading in Fig. 4; [30]). In this regime, increasing the activity of one excitatory neuron results in a decrease of the activity of the other neurons within the column, but is not able to reduce their activity to below the firing threshold. If excitation is strengthened, a regime of hard competition is reached (hWTA), whereby only a single excitatory neuron can be active at a given time. If inhibition is

made too weak, then activity within a column becomes unbalanced and saturates, and no competition is possible (UN). 167 168
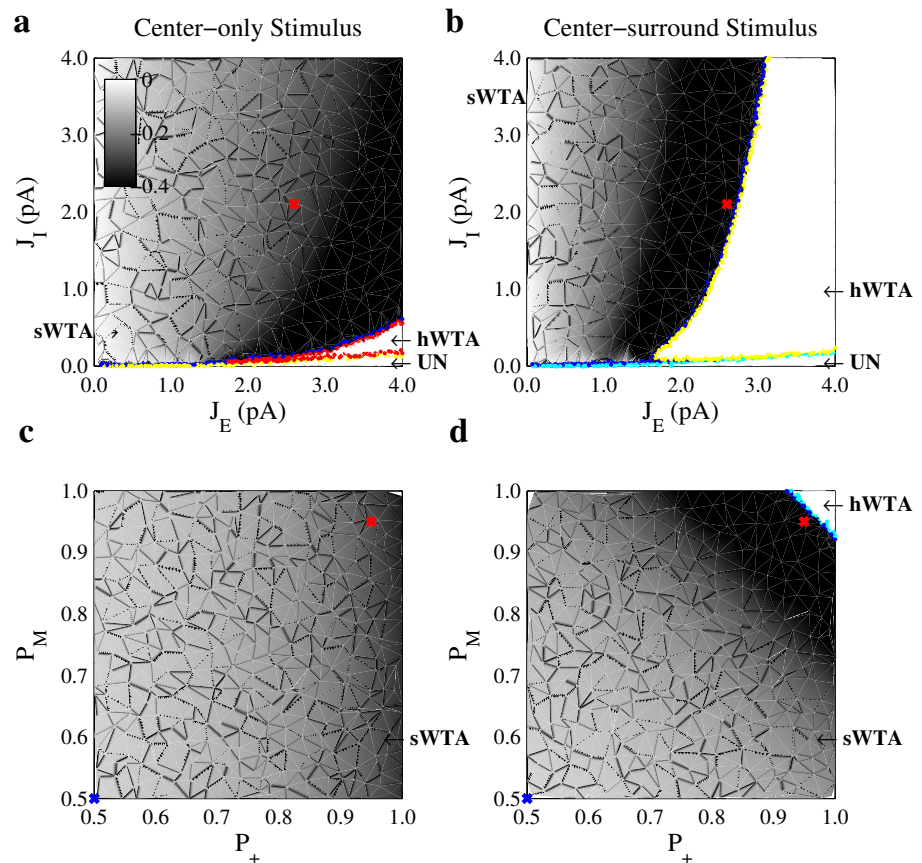

Figure 4. Dependence of competition on stimulation type and model parameters. Both synaptic strength (**a–b**; inhibitory: J_I; excitatory: J_E) and degree of SSN-specificity (**c–d**; local: P_+; long-range: P_M) affect the strength of competition within a column (negative competition index; grey shading. See Methods). Centre-surround stimulation (b and d) generally increases the strength of competition. Both soft and hard competitive regimes exist. sWTA: soft winner-take-all (WTA) regime; hWTA: hard WTA regime; UN: unbalanced regime.

Providing wide-field input to center and surround modules strengthens and changes the profile of competition within a column. For a given choice of parameters, competitive interactions are strengthened by surround stimulation (compare CI at red crosses in Fig. 4a and b; c and d). This occurs simultaneously with a shifting of the parameter regions of the model, such that the size of the region of hard competitive interactions is increased (Fig. 4b). Consistent with competition being responsible for reduced correlation in the spiking model, the strength of competition was related to the degree of local and long-range non-random connectivity (P_+ and P_M; Fig. 4c and d). 169 170 171 172 173 174 175 176

Local competition coupled with tuned long-range connections explains orientation-tuned surround suppression

In visual cortex, the strength of suppression induced by wide-field grating stimulation depends on the relative orientations of the grating stimuli presented in the cRF and in the visual surround [51, 53, 55, 57]. We examined the tuning of suppression in our model by simulating the presentation of two gratings to the centre and surround populations, while varying the relative stimulus orientations (Fig. 5). Consistent with experimental findings, the strongest suppression occurred in our model when the orientations of the center and surround stimuli were aligned ($\Delta\theta = 0$; Fig. 5a and b).
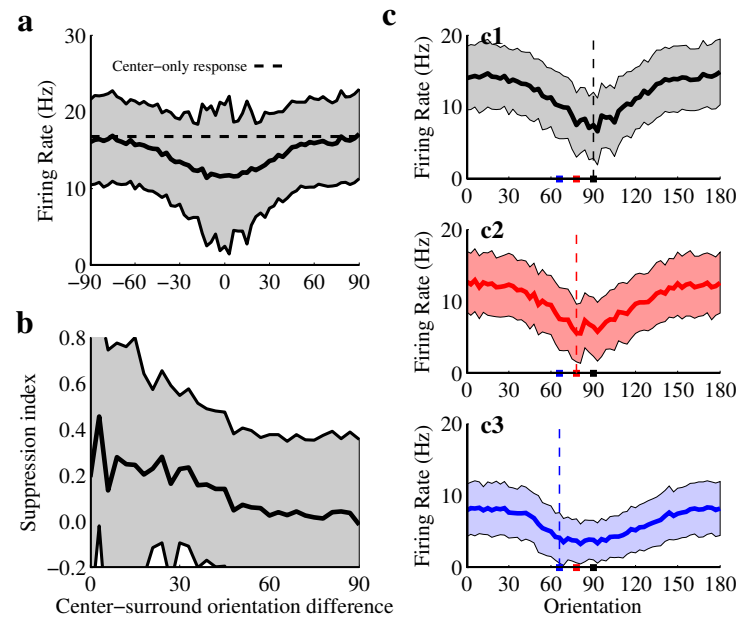

Figure 5. Orientation-tuned suppression under centre-surround stimulation. (a)
Centre-surround grating stimulation (black line: mean response; shading: std. dev.) provokes suppression on average, compared with centre-only stimulation (dashed line: response for centre-only stimulation at preferred orientation). **(b)** In agreement with experimental findings, our model exhibits orientation-tuned suppression that is strongest when centre and surround orientations are aligned [51, 53, 55]. **(c)** Responses of neurons preferring vertical gratings (90°) that exhibit suppression under center-surround stimulation with gratings (orientation of surround stimulus indicated on x-axis). Mean response (thick lines) and standard deviations (shading) are shown. The profile of suppression shifts depending on the orientation presented to the cRF (colours of curves corresponding to pips at bottom, indicating orientation of cRF stimulus). The orientation that provokes maximum surround suppression depends on the orientation presented to the classical receptive field of a neuron; not on the preferred orientation of that neuron [57].

Somewhat surprisingly, experimental results show that the orientation tuning of surround suppression in visual cortex is not locked to the preferred orientation (θ_0) of the neuron under examination [57]. If a non-optimal stimulus (θ_n) is presented in the cRF, then the strongest suppression occurs when the grating orientation presented in the surround matches the non-optimal stimulus (θ_n), rather than the neuron's preferred orientation (θ_0). This phenomena

results in a progressive shift of the surround suppression response tuning curve, such that the $\qquad$ 191
minimum of the curve is aligned with the orientation of the stimulus presented in the cRF. $\qquad$ 192

Our model reproduces both these aspects of surround suppression, by combining local $\qquad$ 193
competition with orientation-tuned long-range excitatory connections (see Fig. 5). Note that $\qquad$ 194
long-range excitatory connections are made with no inhibitory bias in our model. That is, $\qquad$ 195
synapses are made onto excitatory and inhibitory targets in proportion to the existence of those $\qquad$ 196
targets in the cortex, as observed experimentally [61]. In our model, 80% of local and $\qquad$ 197
long-range excitatory synapses are made onto excitatory targets (see Methods). Excitatory $\qquad$ 198
synapses are evenly split between local and long-range projections (i.e. $P_{IN}, P_I = 50\%$; see $\qquad$ 199
Methods); this is also in line with experimental observations [62]. $\qquad$ 200

Consistent with experimental findings in columnar visual cortex, the strongest surround $\qquad$ 201
suppression occurs in our model when the stimulus orientation presented in the cRF and in the $\qquad$ 202
visual surround are aligned (Fig. 5a–b). This is because strongest local competition is recruited $\qquad$ 203
when the long-range connections from the visual surround are activated simultaneously with $\qquad$ 204
local input. Responses in our model are suppressed on average under wide-field stimulation (see $\qquad$ 205
Fig. 5a). Due to the competitive mechanism responsible for suppression in our model, one of the $\qquad$ 206
local subnetworks will have stronger activity than the others. As a consequence, a subset of $\qquad$ 207
neurons express facilitation under surround stimulation (suppression index $SI < 0$ in Fig. 5b). $\qquad$ 208
The proportional size of the facilitated population depends on the number of local subnetworks $\qquad$ 209
(four in our model, implying that $1/4$ of excitatory neurons exhibit facilitation). $\qquad$ 210

Our model replicates the phenomenon of maximum suppression shifting with the orientation $\qquad$ 211
presented to the cRF (Fig. 5c; experimental observations in [57]). When non-preferred stimuli $\qquad$ 212
are presented in the cRF (pips in Fig. 5c), the profile of suppression shifts in response such that $\qquad$ 213
strongest suppression occurs when the surround orientation matches the cRF orientation $\qquad$ 214
(colored curves in Fig. 5c). $\qquad$ 215

Local competition explains sparsening of local responses to wide-field natural stimuli
$\qquad$ 216
$\qquad$ 217

Responses of neurons in visual cortex are poorly correlated in response to natural $\qquad$ 218
stimuli [3, 4, 9, 10], and even more negatively correlated in response to wide-field stimulation $\qquad$ 219
compared with cRF-only stimulation [9, 10]. Reduced correlation of responses leads to increased $\qquad$ 220
population sparseness, increasing information coding efficiency of cortex as discussed above. At $\qquad$ 221
the same time, lifetime sparseness also increases with wide-field stimulation [9, 10] — this $\qquad$ 222
further improves the selectivity of neurons in cortex, by ensuring they fire in response to only $\qquad$ 223
few configurations of visual stimuli. It should be noted that population and lifetime sparseness $\qquad$ 224
are not necessarily correlated in populations of neurons [63], meaning that increases in one do $\qquad$ 225
not imply a corresponding increase in the other measure. $\qquad$ 226

We probed our model with simulated natural stimuli, presented either to the central $\qquad$ 227
population only, or as wide-field stimuli (Fig. 6). Responses of a column of neurons to $\qquad$ 228
center-only stimulation were significantly less correlated than the correlations present in the $\qquad$ 229
input stimulus, measured by recording the responses of a control network with no recurrent $\qquad$ 230
connectivity (Fig. 6c; med. correlation coefficients 0.59 vs 0.63; $P < 10^{-10}$, rank-sum test, $\qquad$ 231
4 neurons $\times$ 60 columns $\times$ 15 trials). However, wide-field stimulation further reduced response $\qquad$ 232
correlations within a column (med. correlation 0.28; $P \approx 0$ versus centre-only stimulation, $\qquad$ 233
rank-sum test, 4 neurons $\times$ 60 columns $\times$ 15 trials). This decorrelation led to a significant $\qquad$ 234
increase in population sparseness in response to wide-field stimulation (Fig. 6d; med. $\qquad$ 235
sparseness 0.11 vs 0.62; $P \approx 0$, rank-sum test, 240 neurons $\times$ 15 trials), consistent with $\qquad$ 236
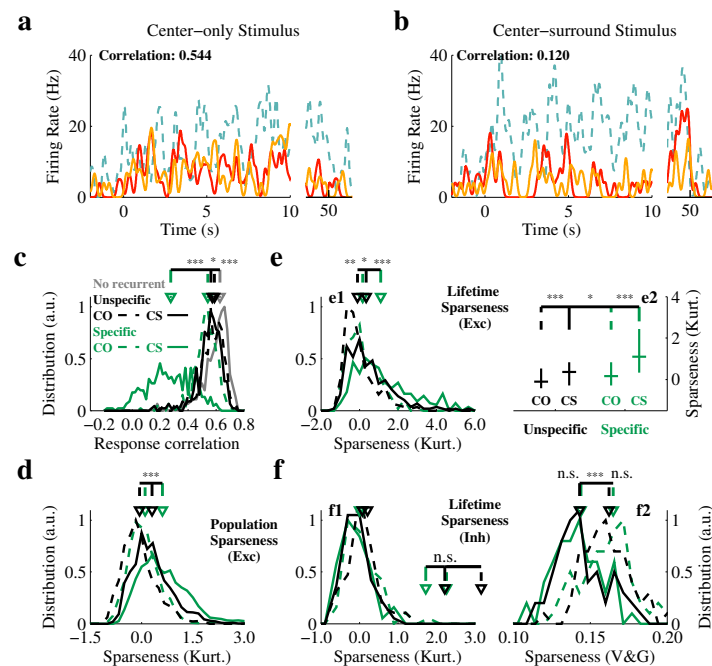experimental observations [4, 9]. $\qquad$ 237

Figure 6. Sparsening of responses to simulated natural stimuli. (a–b) Firing rate profiles in response to cRF-only (a) and wide-field natural stimuli (b). Colors are as indicated in Fig. 2a–d. Firing rate curves show the responses of neurons tuned for 90° orientation, as indicated in a and b. See Methods for a description of the time-varying natural stimulus. **(c–e)** Wide-field stimulation provokes a significant reduction in correlations within the local population (c), reflected in a significant increase in both population (d) and lifetime sparseness (e). Colors and curve styles as indicated in (e2). **(f)** Responses of the inhibitory population to wide-field stimulation are significantly elevated, and are less sparse under the Vinje-Gallant measure (right; V&G) but not under a kurtosis measure (left; Kurt.). Inset: statistical comparison for (f1). Stronger and less sparse inhibitory responses have been observed experimentally [9, 10]. "Specific": full network. "Unspecific": network without local competition in c–f, $P_+ = P_M = 25\%$, with other parameters unchanged. "No recurrent": network with all recurrent connections removed, $J_E = J_I = 0$. a.u.: arbitrary units. Horizontal bars indicate significance; n.s.: not significant, $p > 0.05$; * $p < 0.05$; *** $p < 0.001$.

The response selectivity of excitatory neurons, measured by lifetime sparseness, was also increased in our model under wide-field stimulation (Fig. 6e; med. sparseness 1.10 vs 0.17; $P \approx 0$, rank-sum test, 240 neurons × 15 trials), also consistent with experimental observations [4, 9, 10]. This increase in excitatory selectivity came at the cost of inhibitory selectivity (Fig. 6f). Inhibitory activity was increased on average between cRF and wide-field stimulation (mean response 15.5 vs 18.3 Hz; $P \approx 0$, t-test, 60 neurons), and lifetime sparseness decreased slightly but not significantly under the kurtosis measure and decreased significantly under the Vinje-Gallant measure (med. sparseness 0.14 vs 0.17; $P < 10^{-7}$, rank-sum test, 60 neurons × 15 trials; see Methods). This inverse relationship between excitatory and inhibitory selectivity is consistent with experimental observations [10].

Discussion

We constructed a model for columnar visual cortex, designed to explore integration of information from the visual surround. Our architecture is consistent with the known meso-scale architecture of columnar cortex, which is characterised by long-range, functionally specific (i.e. orientation specific) lateral excitatory projections coupled with short-range local inhibition [8, 10, 49, 64, 65]. We include excitatory specificity over a set of local excitatory subnetworks (SSN-specificity) in order to explore the effect of local competition within a cortical column [8].

Local competition versus inhibitory specificity   Several previous models of surround visual interactions have proposed alternative mechanisms for surround suppression. Schwabe and colleages explained the suppressive effects of far surround visual stimulation through fast axonal transport over inter-areal connections [66], but did not examine orientation tuning of surround suppression. They also require that long-range excitatory projections preferentially target inhibitory neurons, which is not justified by anatomical studies of columnar visual cortex [67] but which may underlie a portion of surround suppression in the rodent [68]. Shushruth and colleagues proposed a model that reproduces the fine orientation tuning of surround suppression [57], which relies on strongly tuned feedforward inhibition from the visual surround in a hand-crafted inhibitory network. Several other models for surround suppression (e.g. Somers and colleagues [69]; Stetter and colleagues [70]; Rubin and colleagues [71]) assume horizontally-expressed inhibition on the spatial scale of orientation hypercolumns – a region of the cortical surface spanning all preferred orientations, corresponding to around 1 mm in cat primary visual cortex. However, competition on this scale is poorly supported by cortical anatomy [8].

In our model, suppression provoked by surround stimulation arises through a *local* competitive mechanism, mediated by strong inhibition within the cortical column balancing local and long-range excitation [62, 72]. Competition arises from local SSN-specific excitatory and non-SSN-specific inhibitory recurrent connections, and is recruited by SSN- and θ-specific long-range excitatory to excitatory (E→E) projections. As a result, the strongest competition — and as a corollary, the strongest suppression — is elicited when the center and surround visual fields are stimulated with gratings of the same orientation. Recruitment of local competition via orientation-tuned E→E connections elicits the shift of suppression with cRF orientation observed experimentally [57]. Importantly, long-range excitatory projections in our model are not class-specific; they target excitatory and inhibitory neurons according to their proportions in the cortex.

Sharpening of responses; correlation and information   In our model, competition leads to sharpening of response preferences (i.e. increased lifetime sparseness) as well as reducing correlations in activity across the local population (i.e. increased population sparseness), implying that more information about the stimulus is transmitted by each spike. Competition therefore reduces correlation in the sense of signal correlation, which did not occur in a network with local connectivity modified to remove competition (Fig. 6c). Inhibitory feedback loops, which are abundant in cortical networks, efficiently reduce correlations in neuronal activity, to the extent that neurons receiving identical presynaptic input can fire nearly independently [24, 26, 73].

Using this architecture of specific excitation and non-specific inhibition, our model reproduces many features of visual responses related to surround integration, such as orientation-tuned surround suppression and sparsening of excitatory responses under wide-field stimulation. In addition, local competition between neurons within a column in our model

explains the surprisingly low noise correlations between neighbouring neurons in columnar visual cortex [3, 5].

Natural stimuli are extremely redundant [13, 14]. If responses of neurons in visual cortex reflected this redundancy by simply relaying input stimuli, then the information transmitted per neural spike would be low (i.e. a non-sparse encoding). Instead, responses in visual cortex are decorrelated or anticorrelated, implying the presence of a neuronal or network mechanism that reduces correlations in response to visual stimuli. Some temporal whitening may take place at the level of the retina or LGN [74], and some low-level reduction of spatial correlation is implemented by surround inhibition in the retina [75, 76] and dLGN [77]. However, active correlation reduction of nearby neurons in cortex with similar orientation preference, or between cortical neurons distributed across visual space, cannot occur in either the retina or dLGN. Stimulation of the visual surround leads to increased response sparseness and therefore improved coding efficiency from an information-theory perspective, possibly to reduce the deleterious effect of natural stimulus redundancy [78].

Competition and response suppression   Due to the presence of local competition in our model, the majority of neurons within a column will show suppression at any given time. As a corollary, some minority of neurons will show facilitation in response to surround stimulation (the "winners" of the competition). In fact, the proportion of facilitating neurons is directly related to the number of local network partitions that are in competition and to the strength of competition. This result implies that experimental quantification of the proportion of facilitation will provide a direct estimate of that parameter of network connectivity. In our model, only a single subnetwork can win the competition; all other subnetworks are suppressed. Therefore, the proportion of neurons undergoing facilitation will converge to $1/M$, where $1/M$ is an estimate of the size of a local subnetwork and M is an estimate for the number of local subnetworks. This parameter can be estimated directly from in vivo recordings of facilitation and suppression under centre-only and full-field visual stimulation, as long as neurons are roughly evenly distributed between local subnetworks in cortex.

Formation of local and long-range specificity   Our model assumes that local excitatory neurons form ensembles within which recurrent connections are made more strongly, called specific subnetworks or "SSNs". Patterns of local connectivity consistent with a subnetwork architecture have been described in rodent cortex [32, 34, 41, 48, 49], but have not been examined in animals with columnar visual cortices. Nevertheless, plastic mechanisms within recurrently connected networks of excitatory and inhibitory neurons lead to partitioning of the excitatory network into ensembles [79]. This process occurs during development in rodent cortex after the onset of visual experience [80]; we suggest that similar fundamental plastic mechanisms could apply in columnar visual cortex.

Long-range horizontal connections develop in several stages in cat area 17. Initial sparse outgrowth is followed by pruning and increasingly dense arborisation [81], with the result that regions of similar orientation preference are connected [7, 47]. The mechanism for surround suppression exhibited by our model is strongly expressed when long-range excitatory projections between two distant populations preferentially and reciprocally cluster their synapses within individual SSNs in the two populations (i.e. $P_M > 0.5$; see Figs 3 and 4). Note that the precise identity of the two SSNs is not crucial; for simplicity we give them the same index in our model.

We propose that specific targetting of long-range projections could come about through similar mechanisms described above for local partitioning of cortex into SSNs. Initially, long-range projections would be made nonspecifically, across SSNs. However, the tendency for local populations to compete will lead to the activity of individual SSNs to be out of phase with each other. SSNs that happen to be concurrently active in two distant populations will induce

reciprocal clustering of long-range projections between the two SSNs in the two populations. Concurrently active SSNs will therefore begin to encourage each other's activity, leading to stronger clustering of long-range projections.

<div align="center">⊰</div>

Competitive mechanisms are known to promote sparse coding [82, 83]; we showed that the architecture of columnar visual cortex lends itself well to local competition as a fundamental computational mechanism for cortex. Local competition can be recruited by excitatory influences from the visual surround to increase response selectivity; this mechanism explains many features of surround visual stimulation in columnar visual cortex. Local excitatory SSN-specificity, over and above connection preference for similar preferred orientations, has not been sought experimentally in mammals with columnar cortices, although it is is important for shaping visual responses in rodent cortex [49]. Our results suggest that careful experimental quantification of local circuitry, in functionally-identified neurons, will be important to identify the mechanisms of surround integration in columnar cortex.

Materials and Methods

The spiking center-surround model

All parameters used for the spiking simulations are summarised in Table 1.

Neuron model   Excitatory (E; exc.) and inhibitory (I; inh.) neurons are modeled as leaky integrate-and-fire neurons [84], characterized by a resting potential $V_L = -70$ mV, a firing threshold $V_{\text{th}} = -50$ mV and a reset potential $V_{\text{reset}} = -55$ mV. The subthreshold membrane potential dynamics $V_{E,I}(t)$ evolve under the differential equation

$$C_m \frac{\mathrm{d}V(t)}{\mathrm{d}t} = -g_L\left[V(t) - V_L\right] - I_{syn}(t), \tag{1}$$

where the membrane capacitance $C_m = 0.5$ nF for excitatory neurons and $C_m = 0.2$ nF for inhibitory neurons; the leak conductance $g_L = 25$ nS for excitatory neurons and $g_L = 20$ nS for inhibitory neurons. After firing, the membrane potential C_m is reset to V_{reset} and held there for a refractory period of τ_{ref} seconds. Refractory periods are $\tau_{\text{ref}} = 2$ ms for excitatory neurons and $\tau_{\text{ref}} = 1$ ms for inhibitory neurons. $I_{\text{syn}}(t)$ denotes the total synaptic input current.

Synaptic interactions   Excitatory postsynaptic currents (EPSCs; I_E); inhibitory postsynaptic currents (IPSCs; I_I); excitatory input currents arising from external network input (I_{Ext}); and noisy background synaptic inputs (I_{Back}) are modelled as

$$I_E(t) = g_E\left[V(t) - V_{\text{rev}}^E\right]\sum_s n_s \cdot S_{E,s}(t), \tag{2}$$

$$I_I(t) = g_I\left[V(t) - V_{\text{rev}}^I\right]\sum_s n_s \cdot S_{I,s}(t), \tag{3}$$

$$I_{\text{Ext}}(t) = g_{\text{Ext}}\left[V(t) - V_{\text{rev}}^E\right] S_{\text{Ext}}(t) \text{ and} \tag{4}$$

$$I_{\text{Back}}(t) = g_{\text{Back}}\left[V(t) - V_{\text{rev}}^E\right] S_{\text{Back}}(t) \tag{5}$$

respectively, where the sums are over the set of input synaptic gating variables S_*; n_s is the number of synapses formed in a particular connection; and the reversal potentials are given

by $V_{\text{rev}}^E = 0\,\text{mV}$ and $V_{\text{rev}}^I = -70\,\text{mV}$. The synaptic gating variables $S_*(t)$ evolve in response to an input spike train of spike time occurrences t_p, under the dynamics

$$\frac{dS_*(t)}{dt} = -\frac{S_*(t)}{\tau_*} + \sum_p \delta\left(t - t_p\right). \tag{6}$$

Here τ_* are time constants of synaptic dynamics, and are given by $\{\tau_E, \tau_I, \tau_{\text{Ext}}, \tau_{\text{Back}}\} = \{5\,\text{ms}, 20\,\text{ms}, 2\,\text{ms}, 2\,\text{ms}\}$ for excitatory, inhibitory, external and background synapses, respectively. Note that axonal conduction times are not considered, such that network interactions are considered to be instantaneous. Synaptic peak conductances g_* are class- and pathway-specific, and are defined in more detail below.

Network architecture   The centre-surround model network consists of several populations $i \in [1 \ldots N]$, each representing a hypercolumn of cat primary visual cortex (area 17; see Fig. 1). For the sake of simplicity we choose only seven populations in this work, i.e. $N = 7$. As such, each population i contains several columns, with each column k corresponding to a preferred orientation θ_k, where $\theta_k \in [0 \ldots 180°]$ and $k \in [1 \ldots N_{\text{Col}}]$, such that $\theta_k = (k-1)\,180/N_{\text{Col}}$. We take $N_{\text{Col}} = 60$ in this paper. In addition, excitatory neurons within each column are partitioned into a set of M subnetworks indexed with $j \in [1 \ldots M]$. For simplicity, a single excitatory neuron is defined per subnetwork, such that no additional index is needed to distinguish neurons within the same subnetwork. Only a single inhibitory neuron is present in each column θ_k.

Within a single population i, synaptic connections are modulated by similarity of preferred orientation $\Delta\theta$, which has a one-to-one mapping with physical cortical space under the transformation $180° \approx 1\,\text{mm}$ [47]. To avoid edge effects in our model we adopt a circular topology of preferred orientations θ, with a periodicity of $180°$. $\Delta\theta$ is therefore defined as the minimum distance around a ring according to the relative orientation preference of two neurons; that is, $\Delta\theta = \min(|\theta_1 - \theta_2|, 180 - |\theta_1 - \theta_2|)$.

Both local (within-population) and long-range (between-population) excitatory connections are modulated by similarity in orientation preference between source and target neurons ($\Delta\theta$), as well as by whether or not the source and target neurons share subnetwork membership j. For orientation-specific connectivity, we use a Gaussian function over $\Delta\theta$, given by

$$\mathscr{G}(\Delta\theta, \sigma_\theta) = \frac{180}{\sqrt{2\pi} \cdot N_{\text{Col}} \cdot \sigma_\theta} \exp\left(\frac{-\Delta\theta^2}{2\sigma_\theta^2}\right). \tag{7}$$

Excitatory and inhibitory synapses are distributed over connection pathways under a set of functions $n_*(i_1, i_2, j_1, j_2, \Delta\theta)$, which define the number of synapses made between any two neurons. These functions for recurrent excitatory connectivity are defined as

$$n_{E \to E}(i_1 = i_2, j_2 = j_2, \Delta\theta) = P_{\text{IN}} \cdot P_+ \cdot f_E \cdot N_{\text{Syn,E}} \cdot \mathscr{G}\left(\Delta\theta, \sigma_E^{\text{Local}}\right) \tag{8}$$

$$n_{E \to E}(i_1 \neq i_2, j_2 = j_2, \Delta\theta) = (1 - P_{\text{IN}})\,P_M \cdot f_E \cdot N_{\text{Syn,E}} \cdot \mathscr{G}\left(\Delta\theta, \sigma_E^{\text{Long}}\right) \Big/ (N-1) \tag{9}$$

$$n_{E \to E}(i_1 = i_2, j_2 \neq j_2, \Delta\theta) = P_{\text{IN}}\,(1 - P_+)\,f_E \cdot N_{\text{Syn,E}} \cdot \mathscr{G}\left(\Delta\theta, \sigma_E^{\text{Local}}\right) \Big/ (M-1) \tag{10}$$

$$n_{E \to E}(i_1 \neq i_2, j_2 \neq j_2, \Delta\theta) = (1 - P_{\text{IN}})\,(1 - P_M)\,f_E \cdot N_{\text{Syn,E}} \cdot \mathscr{G}\left(\Delta\theta, \sigma_E^{\text{Long}}\right) \Big/ (N-1)(M-1) \tag{11}$$

These functions define rules for excitatory connections that are local and within the same SSN (Eq. 8); long-range and within the same SSN (Eq. 9); local across different SSNs (Eq. 10); and long-range across different SSNs (Eq. 11) respectively. Connection fields are modulated by

parameters σ_*; "Local" denotes connections within the same population and "Long" denotes connections between populations.

Note that a fraction $P_{\text{IN}} \in [0\dots1]$ of excitatory synapses are formed locally, and the remainder are distributed across the $N-1$ other populations. Similarly, fractions $P_+ \in [0\dots1]$ and $P_M \in [0\dots1]$ of excitatory synapses are formed within the same SSN, while the remainder are distributed across the $M-1$ other SSNs; P_+ controls local subnetwork-specificity, while P_M controls long-range subnetwork specificity.

Similarly, connectivity functions involving inhibitory neurons are defined as

$$n_{E \to I}(i_1 = i_2, \Delta\theta) = P_I \cdot f_I \cdot N_{\text{Syn,E}} \cdot \mathscr{G}\left(\Delta\theta, \sigma_E^{\text{Local}}\right) \tag{12}$$

$$n_{E \to I}(i_1 \neq i_2, \Delta\theta) = (1 - P_I) \cdot f_I \cdot N_{\text{Syn,E}} \cdot \mathscr{G}\left(\Delta\theta, \sigma_E^{\text{Long}}\right) / (N - 1) \tag{13}$$

$$n_{I \to E}(\Delta\theta) = f_E \cdot N_{\text{Syn,I}} \cdot \mathscr{G}(\Delta\theta, \sigma_I) / M \tag{14}$$

$$n_{I \to I}(\Delta\theta) = f_I \cdot N_{\text{Syn,I}} \cdot \mathscr{G}(\Delta\theta, \sigma_I) \tag{15}$$

These functions define $E \to I$ connections made within (Eq. 12) and between (Eq. 13) populations; $I \to E$ connections (Eq. 14); and recurrent inhibitory connections (Eq. 15). Note that $P_I \in [0\dots1]$ excitatory synapses are made with local inhibitory targets, with the remainder made with long-range inhibitory targets. In addition, connections involving inhibitory neurons are θ-specific but not subnetwork-specific, and inhibitory projections are made only locally (i.e. within the same population).

We therefore define $I_{\text{Syn},E}(i, j, \theta_k, t)$ as the total synaptic current input to the excitatory neuron in population i, subnetwork j, with preferred orientation θ_k, at time t. Similarly, we define $I_{\text{Syn},I}(i, \theta_k, t)$ as the total synaptic current input to the inhibitory neuron in population i, in the column with preferred orientation θ_k. Input currents $I_{\text{Syn},*}$ are of the form

$$I_{\text{Syn},*} = I_*^{\text{Local}} + I_*^{\text{Long}} + I_{\text{Ext} \to *} + I_{\text{Back} \to *}, \tag{16}$$

where "Ext" denotes external inputs provides as stimuli to the network; and "Back" denotes background inputs representing spontaneous activity. Each term in Eq. 16 evolves according to the synaptic dynamics in Eq. 5, weighting input from the rest of the network according to the connectivity functions Eqs 8–15.

Background noise and stimulation protocol All neurons receive an excitatory background noise input, modeled as independent Poisson spike trains at a rate of $v_{\text{Back} \to E} = 180\,\text{Hz}$ for excitatory neurons and $v_{\text{Back} \to I} = 50\,\text{Hz}$ for inhibitory neurons.

Our model of cat primary visual cortex (area 17) is designed to explore the computational effects of long-range synaptic input from the visual surround on local representations of orientation preference in the superficial layers of cortex. We therefore assume that orientation preference itself is computed within layer 4, and that inputs to the neurons in the superficial layers are already tuned for orientation.

We simulated external visual stimuli as independent Poison spike trains. For oriented grating stimuli, the rate $v_{\text{Grat}}(\theta_k, t)$ of the input spike trains received by both excitatory and inhibitory neurons depended on the preferred orientation θ_k of the neuron and the instantaneous stimulus orientation $\theta_{\text{Grat}}(t)$, under

$$v_{\text{Grat}}(\theta_k, t) = \alpha_{\text{Grat}} \cdot h(t) \exp\left[-\frac{\Delta\theta(\theta_k, \theta_{\text{Grat}}(t))^2}{\sigma_{\text{Grat}}^2}\right], \tag{17}$$

Table 1. Parameters used in simulations of the spiking model. Exc., E: excitatory / excitation; Inh., I: inhibitory / inhibition; Prop.: proportion of; Syn.: synapses; SSN: Specific subnetwork.

Parameter	Description	Value
V_L	Neuron resting potential	$-70\,\text{mV}$
V_{th}	Neuron firing threshold voltage	$-50\,\text{mV}$
V_{reset}	Neuron reset voltage	$-55\,\text{mV}$
$C_{m,E}$; $C_{m,I}$	Exc. and Inh. neuron membrane capacitance	0.5 nF; 0.2 nF
$g_{L,E}$; $g_{L,I}$	Exc. and Inh. neuron leak conductance	25 nS; 20 nS
$\tau_{\text{ref},E}$; $\tau_{\text{ref},I}$	Exc. and Inh. neuron refractory periods	2 ms; 1 ms
$g_{E\to E}$; $g_{E\to I}$; g_I	$E \to E$, $E \to I$ and Inh. syn. conductances	0.05 nS; 0.2 nS; 0.12 nS
g_{Ext}	Synaptic conductance for external inputs	11.43 nS
g_{Back}	Synaptic conductance for spontaneous inputs	11.43 nS
V_{rev}^E; V_{rev}^I	Exc. and Inh. syn. reversal potentials	0 mV; $-70\,\text{mV}$
τ_E; τ_I; τ_{Ext}; τ_{Back}	Time constants governing syn. dynamics	5 ms; 20 ms; 2 ms; 2 ms
N	Number of populations (hypercolumns)	7
N_{Col}	Number of columns in each population	60
M	Number of subnetworks (SSNs)	4
f_E	Prop. syn. made by all neurons onto Exc. targets	80%
f_I	Prop. syn. made by all neurons onto Inh. targets	20%
P_{IN}	Prop. E→E syn. made locally	50%
P_+	Prop. local E→E syn. reserved to be made within the same SSN	95%
P_M	Prop. long-range E→E syn. reserved to be made within the same SSN	95%
P_I	Prop. E→I syn. made locally, versus long-range E→I projections	50%
σ_E^{Local}; σ_E^{Long}; σ_I	Functional tuning of orientation-specific connections	20°; 20°; 20°
$N_{\text{Syn},E}$; $N_{\text{Syn},I}$	Total syn. made by each exc. or inh. neuron	3000; 4500

where $\sigma_{\text{Grat}} = 27°$ is the tuning sharpness of orientation-tuned inputs, and $\Delta\theta$ describes orientation differences around the ring topology as described above. The amplitude of stimulus input $\alpha_{\text{Grat}} = 270\,\text{Hz}$ and $29\,\text{Hz}$ for excitatory neurons and inhibitory neurons, respectively. During center-only visual stimulation, $h(t) = 1$ for the center population and 0 for surround populations. During center-surround stimulation, $h(t) = 1$ for both center and surround populations.

The simulated natural stimulus was generated as a complex pattern of varying oriented input over the visual field, which shifted over time. Neurons within the same column received similar input $v_{\text{Nat}}(\theta_k, t)$, by virtue of their shared orientation preference, depending on the difference between the orientation of the stimulus $\theta_{\text{Nat},k}$ and their preferred orientation θ_k, under

$$v_{\text{Nat}}(\theta_k, t) = h(t) \left\{ v_{\text{const}} + \alpha_{\text{Nat}} \exp \left[-\frac{\Delta\theta(\theta_k, \theta_{\text{Nat},k}(t))^2}{\sigma_{\text{Nat}}^2} \right] \right\}, \qquad (18)$$

where $\sigma_{Nat} = 20°$. In columnar visual cortex, neighbouring neurons are likely to receive less correlated input than this, due to relative shifts in receptive field location. However since the goal of our model is to investigate local competition and reduction of correlations, we designed our stimulus to contain local correlations. During center-only visual stimulation (0 s to 50 s), $h(t) = 1$ and 0 for the center and surround hypercolumns, respectively. During center-surround stimulation $h(t) = 1$ for both hypercolumns. $\alpha_{Nat} = 40\,\text{Hz}$ and $0\,\text{Hz}$ for excitatory neurons and inhibitory neurons, respectively, while $v_{\text{const}} = 148\,\text{Hz}$ and $29\,\text{Hz}$ for excitatory neurons and inhibitory neurons, respectively.

The stimuli provided to each column $\theta_{\text{Nat},k}(t)$ for both center and surround populations were generated by spatially and temporally filtering independent white noise signals for each column. An ergodic noise process $\vartheta_k(t)$ was generated for each column, and evolved under the dynamics

$$\vartheta_k(t + \Delta t) = \vartheta_k(t) + \lambda_{\text{noise}}\eta_k(t) \text{ and} \qquad (19)$$

$$\tau_{\text{noise}} \frac{d\eta_k(t)}{dt} = -\eta_k(t) + \sigma_{\text{noise}}\xi(t)\sqrt{\tau_{\text{noise}}}, \qquad (20)$$

where $\tau_{\text{noise}} = 2\,\text{ms}$, $\sigma_{noise} = 0.18°$ and $\xi(t)$ is a gaussian white noise process with zero mean and unit variance. The time step of the stimulation $\Delta t = 0.1\,\text{ms}$; and $\lambda_{\text{noise}} = 20$. These ergodic noise processes were then spatially filtered under the relationships

$$\theta_{\text{Nat},k}(t) = \arctan \left\{ \frac{\sum_{l=1}^{N_{Col}} \sin[\vartheta_l(t)]\, G[\theta_l(t), \theta_k(t)]}{\sum_{l=1}^{N_{Col}} \cos[\vartheta_l(t)]\, G[\theta_l(t), \theta_k(t)]} \right\} \qquad (21)$$

where $G(\theta_l, \theta_k) = A_0 \cdot \exp\left[-\Delta\theta(\theta_l, \theta_k)^2 / 2\sigma_\theta^2\right]$, $A_0 = 0.6$ and $\sigma_\theta = 2°$.

Parameters for the spiking model   Axons of pyramidal neurons in cat visual cortex make a roughly even split of boutons between local and long-range arbors [62], providing estimates for $P_{IN} = 0.5$ and $P_I = 0.5$. Excitatory neurons make $N_{\text{Syn},E} = 3000$ total synapses per excitatory neuron; inhibitory neurons make $N_{\text{Syn},I} = 4500$ total synapses per inhibitory neuron [62, 85]. All neurons in the model connect to excitatory and inhibitory targets roughly in proportion to the prevalence of excitatory and inhibitory neurons in cortex [61]: $f_E = 80\%$ of synapses in the model are made with excitatory targets and $f_I = 20\%$ of synapses are made with inhibitory targets.

Specificity of connections between excitatory neurons has been observed in several cortical areas in the rodent [32, 86, 87], and is correlated with similarity in visual feature preference in

rodent visual cortex [34, 41, 49]. The presence of functionally specific connectivity of the type proposed in this paper has not been investigated in columnar visual cortex (e.g. in cat or monkey), leading us to explore a range of specificity levels P_+ and P_M. We used nominal values of $P_+ = P_M = 95\%$. 476 477 478 479

Since inhibitory responses are similarly tuned as excitatory responses in cat primary visual cortex [88], all σ_θ are $20°$. Since the mapping from orientation to physical distance in the central visual field of cat area 17 is approximately 1 mm per $180°$ hypercolumn, this corresponds to a local anatomical projection field of approximately $450\,\mu m$ width [47]. 480 481 482 483

Nonlinear dynamical analysis of the system stability and steady-state response
484 485

Parameters for the mean-field non-spiking model are give in Table 2. 486

Mean-field dynamics We used mean-field analysis methods to investigate the dynamics of the center-surround model. First, we introduce the activation function for excitatory and inhibitory nodes, defined as [89] 487 488 489

$$r\left[I_{\text{syn}}(t)\right] = \frac{\phi\left[I_{\text{Syn}}(t)\right]}{1 + \tau_{\text{ref}} \cdot \phi\left[I_{\text{Syn}}(t)\right]} \text{ and} \tag{22}$$

$$\phi[I_{\text{Syn}}(t)] = \frac{\gamma \cdot I_{\text{Syn}}(t) - I_T}{1 - \exp\left\{-c\left[\gamma \cdot I_{\text{Syn}}(t) - I_T\right]\right\}}, \tag{23}$$

where $r\left[I_{\text{Syn}}(t)\right]$ is the firing rate of a neuron in response to the instantaneous synaptic input current $I_{\text{Syn}}(t)$; c and γ are the curvature and gain factors of the activation function, respectively. The activation function becomes a linear threshold function with I_T/γ as the threshold current when c is large. τ_{ref} is the refractory period of the neuron, which also determines its maximum firing rate. 490 491 492 493 494

We redefine the synaptic gating variables $S_*(t)$ for excitatory and inhibitory synapses in the mean-field model as [89] 495 496

$$\frac{\mathrm{d}S_*(t)}{\mathrm{d}t} = -\frac{S_*(t)}{\tau_*} + r\left[I_{*,\text{Syn}}(t) + I_{*,\text{Ext}} + I_{*,\text{Back}}\right], \tag{24}$$

in which the total synaptic input currents $I_{*,\text{Syn}}(t)$ are given by 497

$$I_*(t) = J_* \sum_s n_s \cdot S_{*,s}(t), \text{ where} \tag{25}$$

$$J_* = g_* \left[\langle V(t) \rangle - V_{\text{rev}}^*\right], \tag{26}$$

and we assume the average membrane potential for each neuron $\langle V(t) \rangle \approx -52.5\,\text{mV}$. The parameters J_E and J_I therefore represent constant synaptic weights (for excitation and inhibition, respectively), rather than synaptic conductances as in the spiking model. 498 499 500

Reduced model For simplicity, we present only the analysis of a reduced model, such that we consider only two populations ($N = 2$), each containing only two SSNs ($M = 2$) and without considering orientation such that ($N_{\text{Col}} = 1$; see Fig. 1c). The connectivity functions n_* from the spiking model apply as before, but neglecting the indices for preferred orientation. $S_*(t)$ therefore has the form $S_*(t) = [x_{1,1},\ x_{1,2},\ x_{2,1},\ x_{2,2},\ y_1,\ y_2]^T(t)$. Here $x_{i,j}(t)$ is the 501 502 503 504 505

instantaneous value of the gating variable for the excitatory neuron in population i, subnetwork j, and $y_i(t)$ is the value for the inhibitory neuron in population i.

To investigate the dynamics of the mean-field model we calculate the steady-state responses $\bar{S}$ of the system, that is $\bar{S} = S_*(t) : dS_*(t)/dt = 0$. We solve the simplified system in Eq. 24, under centre-only ("CO") or centre-surround ("CS") stimulation, defined as

$$I_{\text{Ext,CO}} = [\iota_E, 0, \iota_E, 0, \iota_I, 0]^T \text{ and} \tag{27}$$

$$I_{\text{Ext,CS}} = [\iota_E, \iota_E, \iota_E, \iota_E, \iota_I, \iota_I]^T, \tag{28}$$

where ι_E and ι_I are stimulation currents delivered to exc. and inh. neurons respectively, to obtain $\bar{S}_{\text{CO}}$ and $\bar{S}_{\text{CS}}$. We then numerically obtain the system Jacobian $J_{\bar{S}_*}$ at these fixed points, and examine the eigenvalues of $J_{\bar{S}_*}$ to determine the stability of the system around these fixed points.

Competition index and computational regimes We also define a competition index ("CI") to quantify the strength of competition exhibited between excitatory neurons in different subnetworks. The competition index measures how strongly the activity of an excitatory neuron in one SSN in the "centre" population is suppressed, when input to the other subnetwork is increased, either for centre-only or centre-surround stimulation. This index is defined as

$$CI \equiv \frac{d\bar{S}_{1,1}}{d\Delta I_C} \tag{29}$$

where ΔI_C defines a perturbation in the input to a selected set of neurons in the network. In the case of centre-only stimulation, $\Delta I_C = [0, 1, 0, 0, 0, 0]^T$; CI therefore quantifies the suppression evoked in the neuron in population 1, SSN 1 by an increase in input to SSN 2 in population 1. That is, population 1 is defined as the "central" population, and we measure competition between SSNs within that population.

In the case of centre-surround stimulation, $\Delta I_C = [0, 1, 0, 1, 0, 0]^T$; CI therefore quantifies the suppression provoked by input to the SSN 2 in both populations 1 and 2. The competition index CI is only defined in the case of stable $\bar{S}$, i.e. when the eigenvalues of $J_{\bar{S}}$ have non-positive real parts.

We use the eigenvalues of $J_{\bar{S}_*}$ in conjunction with the CI to identify parameter regimes of stability and computation (see Fig. 4). If $J_{\bar{S}_*}$ has one or more eigenvalues with positive real part, the system operates in a hard winner-take-all regime ("hWTA"), in which only a single SSN is permitted to be simultaneously active. This is because competition between SSNs is so strong, that activity of a single SSN is capable of entirely suppressing the activity of the other SSNs, via shared inhibitory feedback.

Alternatively, if all eigenvalues of $J_{\bar{S}_*}$ are negative, then the system operates in either a "soft" winner-take-all regime ("sWTA"; if $CI < 0$), such that several simultaneously active SSNs are permitted at steady state, or in a non-competitive regime ("NC"; if $CI > 0$). In the sWTA regime, increasing the external stimulus to one SSN will lead to the decreasing of neural activities of the remaining SSNs, implying competition exists between neurons within a column. Stronger competition is indicated by more negative CI. In the NC regime, however, increasing the input to one SSN will increase the activity of the remaining SSNs. The absence of competition is reflected in a positive CI.

When strong excitation is unbalanced by inhibition, the network is in an "unbalanced" regime ("UN"). This regime is defined as when firing rates of all neurons are close to saturation in the steady state, and all eigenvalues are negative.

Table 2. Parameters used in analysis of the mean-field model that differ from those given in Table 1.

Parameter	Description	Nominal value
c_E; c_I	Exc. and Inh. neuron activation function curvature parameters	160×10^{-3}; 87×10^{-3}
$I_{T,E}/\gamma_E$; $I_{T,I}/\gamma_I$	Exc. and Inh. threshold currents	0.4 nA; 0.2 nA
$\langle V(t) \rangle$	Assumed average membrane potential	-52.5 mV
J_E; J_I	Exc. and Inh. total synaptic weights	2.6 pA; 2.1 pA
N	Number of populations (hypercolumns)	2
N_{Col}	Number of columns in each population	1
M	Number of subnetworks (SSNs)	2
ι_E; ι_I	Input currents representing external stimuli to Exc. and Inh. neurons	0.90 nA; 0.087 nA

Parameters for the firing-rate model We estimated parameters values from experimental measurements of the properties of cortical neurons. The slope of the I–F curve of an adapted cortical pyramidal neuron, corresponding to γ_E in Eqn. 23 is approximately 66 Hz/nA [90]. The corresponding value for basket cells (γ_I) is approximately 351 Hz/nA [91]. The I–F curvature parameters c_E and c_I were chosen to approximate the spiking model. The strength of a single excitatory synapse is estimated by the charge injected into a post-synaptic neuron by a single spike, given by $I_{\text{Syn}} = J_E \cdot S_E(t)$. At steady-state, $S_E(t) = \tau_E$, therefore $J_E = I_{\text{Syn}}/\tau_E$. We estimated nominal values of $J_E = 2.6$ pA and $J_I = 2.1$ pA [92]. We estimated firing thresholds for our neurons of $I_{T,E}/\gamma_E = 0.4$ nA and $I_{T,I}/\gamma_I = 0.2$ nA [90, 91]. The average input currents ι_E and ι_I injected during visual input were estimated from the average currents received by single pyramidal neurons in visual cortex during visual stimulation [90]. We used values of $\iota_E = 0.90$ nA, and a proportional value of $\iota_I = 0.087$ nA [62, 90].

Population and lifetime sparseness measures

The measure of the population sparseness and the life-time sparseness we used mainly is the kurtosis, which measures the 4th moment relative to the variance squared [19] and is given by

$$s_k = \frac{1}{n} \sum_i \frac{(r_i - \bar{r})^4}{\sigma^4} - 3, \tag{30}$$

where r_i is the firing rate of each neuron during the presentation of the ith natural stimulus, and n is the number of natural stimuli frames for lifetime spareness. For population sparseness, r_i is the firing rate of neuron i during a frame of natural stimuli, and n is the number of simultaneously recorded neurons in our model. $\bar{r}$ is the mean firing rate and σ is the standard deviation of the firing rate. For a sparse (i.e. heavy-tailed) distribution, $s_k > 0$.

In addition we used the Vinje-Gallant measure for sparseness, a nonparametric statistic employed previously in [4, 9], given by

$$s_{\text{V\&J}} = \left[1 - \left(\sum_i \frac{r_i}{n} \right)^2 \middle/ \left(\sum_i \frac{r_i^2}{n} \right) \right] \middle/ (1 - 1/n), \tag{31}$$

where $s_{\text{V\&J}} \in [0, 1]$. A larger $s_{\text{V\&J}}$ indicates a more sparse response.

Suppression index

The strength of surround suppression was quantified using a suppression index (SI), which is defined as

$$SI(\theta) = 1 - \frac{R_{CS}(\theta)}{R_{CO}}, \tag{32}$$

where θ is the center-surround orientation difference, R_{CO} is the response to the center-only stimulus, $R_{CS}(\theta)$ is the response to the center-surround stimulus. Therefore, $SI = 1$ indicates that the response in the center population is completely suppressed by the surround stimulus, whereas $SI = 0$ indicates that there is complete lack of suppression from the surround.

Statistical methods

All tests are non-parametric two-sided tests of medians (Wilcoxon Rank Sum), unless stated otherwise.

Supporting Information

Acknowledgments

References

1. Hubel D, Wiesel T. Receptive fields, binocular interaction and functional architecture in the cat's visual cortex. J Physiology. 1962;160:106–54.

2. Hubel DH, Wiesel TN. Receptive fields and functional architecture of monkey striate cortex. Journal of Physiology (London). 1968;195:215–243.

3. Martin KAC, Schröder S. Functional Heterogeneity in Neighboring Neurons of Cat Primary Visual Cortex in Response to Both Artificial and Natural Stimuli. Journal of Neuroscience. 2013;33(17):7325–7344.

4. Yen SC, Baker J, Gray CM. Heterogeneity in the responses of adjacent neurons to natural stimuli in cat striate cortex. Journal of neurophysiology. 2007 Feb;97(2):1326–41. Available from: `http://www.ncbi.nlm.nih.gov/pubmed/17079343`.

5. Ecker AS, Berens P, Keliris Ga, Bethge M, Logothetis NK, Tolias AS. Decorrelated neuronal firing in cortical microcircuits. Science. 2010 Jan;327(5965):584–7. Available from: `http://www.ncbi.nlm.nih.gov/pubmed/20110506`.

6. Martin KAC, Roth S, Rusch ES. Superficial layer pyramidal cells communicate heterogeneously between multiple functional domains of cat primary visual cortex. Nat Commun. 2014;5:5252.

7. Bosking WH, Zhang Y, Schofield B, Fitzpatrick D. Orientation Selectivity and the Arrangement of Horizontal Connections in Tree Shrew Striate Cortex. Journal of Neuroscience. 1997 3;17(6):2112–2127.

8. Muir DR, Cook M. Anatomical constraints on lateral competition in columnar cortical architectures. Neural Computation. 2014 8;26(8).

9. Vinje WE, Gallant JL. Sparse coding and decorrelation in primary visual cortex during natural vision. Science. 2000;287(5456):1273.

10. Haider B, Krause MR, Duque A, Yu Y, Touryan J, Mazer JA, et al. Synaptic and network mechanisms of sparse and reliable visual cortical activity during nonclassical receptive field stimulation. Neuron. 2010 1;65:107–121.

11. Mountcastle VB, Berman AN, Davies PW. Topographic organization and modality representation in first somatic area of cat's cerebral cortex by method of single unit analysis. American Journal of Physiology. 1955;183:646–647.

12. Ecker AS, Berens P, Keliris GA, Bethege M, Logothetis NK, Tolias AS. Decorrelated Neuronal Firing in Cortical Microcircuits. Science. 2010;327:584–587.

13. Kersten D. Predictability and redundancy of natural images. JOSA A. 1987;4(12):2395–2400.

14. Schwartz O, Simoncelli EP; 4 Washington Place Room 809 New York New York 10003 USA. Center for Neural Science. Natural signal statistics and sensory gain control. Nat Neurosci. 2001 8;4(8):819–25.

15. Wiechert MT, Judkewitz B, Riecke H, Friedrich RW. Mechanisms of pattern decorrelation by recurrent neuronal circuits. Nature Neuroscience. 2010 8;13(8):1003–1010.

16. Shamir M, Sompolinsky H. Nonlinear population codes. Neural Computation. 2004;16:1105–1136.

17. Averbeck BB, Latham PE, Pouget A; Department of Brain; Cognitive Sciences; Rochester New York 14627 USA. Center for Visual Science. Neural correlations, population coding and computation. Nat Rev Neurosci. 2006 5;7(5):358–66.

18. Willshaw DJ, Buneman OP, Longuet-Higgins HC. Non-holographic associative memory. Nature. 1969;.

19. Olshausen BA, Field DJ. Sparse coding of sensory inputs. Current opinion in neurobiology. 2004;14(4):481–487.

20. De La Rocha J, Doiron B, Shea-Brown E, Josić K, Reyes A. Correlation between neural spike trains increases with firing rate. Nature. 2007;448(7155):802–806.

21. Hertz J. Cross-correlations in high-conductance states of a model cortical network. Neural Computation. 2010;22(2):427–447.

22. Rosenbaum R, Rubin JE, Doiron B. Short-term synaptic depression and stochastic vesicle dynamics reduce and shape neuronal correlations. Journal of neurophysiology. 2013;109(2):475–484.

23. Bernacchia A, Wang XJ. Decorrelation by recurrent inhibition in heterogeneous neural circuits. Neural computation. 2013;25(7):1732–1767.

24. Helias M, Tetzlaff T, Diesmann M. The Correlation Structure of Local Neuronal Networks Intrinsically Results from Recurrent Dynamics. PLoS computational biology. 2014;10(1):e1003428.

25. Renart A, de la Rocha J, Bartho P, Hollender L, Parga N, Reyes A, et al. The asynchronous state in cortical circuits. science. 2010;327(5965):587–590.

26. Tetzlaff T, Helias M, Einevoll GT, Diesmann M. Decorrelation of neural-network activity by inhibitory feedback. PLoS computational biology. 2012 Aug;8(8):e1002596.

27. Pernice V, Staude B, Cardanobile S, Rotter S. How structure determines correlations in neuronal networks. PLoS computational biology. 2011;7(5):e1002059.

28. Coultrip R, Granger R, Lynch G. A cortical model of winner-take-all competition via lateral inhibition. Neural Networks. 1992;5(1):47–54.

29. Douglas RJ, Mahowald MA, Martin KAC. Hybrid analog-digital architectures for neuromorphic systems. In: Proc. IEEE World Congress on Computational Intelligence. vol. 3. IEEE; 1994. p. 1848–1853.

30. Douglas RJ, Martin K. Recurrent neuronal circuits in the neocortex. Current Biology. 2007;17(13):R496–R500.

31. Rutishauser U, Douglas R. State-Dependent Computation Using Coupled Recurrent Networks. Neural Comput. 2009;21:478–509.

32. Yoshimura Y, Dantzker JLM, Callaway EM. Excitatory cortical neurons form fine-scale functional networks. Nature. 2005 2;433:868–873.

33. Lefort S, Tomm C, Floyd Sarria JCC, Petersen CCH. The excitatory neuronal network of the C2 barrel column in mouse primary somatosensory cortex. Neuron. 2009 1;61(2):301–16.

34. Ko H, Hofer SB, Pichler B, Buchanan KA, Sjöström PJ, Mrsic-Flogel TD. Functional specificity of local synaptic connections in neocortical networks. Nature. 2011;473:87–91.

35. Ishikawa AW, Komatsu Y, Yoshimura Y. Experience-dependent emergence of fine-scale networks in visual cortex. J Neurosci. 2014 9;34(37):12576–86.

36. Matsuzaki M, Ellis-Davies GC, Kasai H. Three-dimensional mapping of unitary synaptic connections by two-photon macro photolysis of caged glutamate. Journal of neurophysiology. 2008;99(3):1535–1544.

37. Boucsein C, Nawrot M, Schnepel P, Aertsen A. Beyond the cortical column: abundance and physiology of horizontal connections imply a strong role for inputs from the surround. Frontiers in neuroscience. 2011;5:32.

38. Martin KA. Neuroanatomy: Uninhibited Connectivity in Neocortex? Current Biology. 2011;21(11):R425–R427.

39. Fino E, Yuste R. Dense Inhibitory Connectvity in Neocortex. Neuron. 2011;69:1188–1203.

40. Bock DD, Lee WCACA, Kerlin AM, Andermann ML, Hood G, Wetzel AW, et al. Network anatomy and in vivo physiology of visual cortical neurons. Nature. 2011 3;471:177–182.

41. Hofer SB, Ko H, Pichler B, Vogelstein J, Ros H, Zeng H, et al.; Physiology Department of Neuroscience; London UK. Pharmacology. Differential connectivity and

response dynamics of excitatory and inhibitory neurons in visual cortex. Nat Neurosci. 2011 8;14(8):1045–52.

42. Mariño J, Schummers J, Lyon DC, Schwabe L, Beck O, Wiesing P, et al. Invariant computations in local cortical networks with balanced excitation and inhibition. Nature Neuroscience. 2005;8(2):194–201.

43. Gilbert CD, Wiesel TN. Columnar Specificity of Intrinsic Horizontal and Cortico-Cortical Connections in Cat Visual Cortex. JNeurosci. 1989;9:2432–2442.

44. Malach R, Amir Y, Harel M, Grinvald A. Relationship between intrinsic connections and functional architecture revealed by optical imaging and in vivo targeted biocytin injections in primate striate cortex. Proc Natl Acad Sci USA. 1993 11;90:10469–10473.

45. Yoshioka T, Blasdel GG, Levitt JB, Lund JS. Relation between patterns of intrinsic lateral connectivity, ocular dominance, and cytochrome oxidase-reactive regions in macaque monkey striate cortex. Cerebral Cortex. 1996 3;6:297–310.

46. Muir DR, Douglas R. From neural arbors to daisies. Cerebral Cortex. 2011 5;21(5):1118–1133.

47. Muir DR, Da Costa NMA, Girardin CC, Naaman S, Omer DB, Ruesch E, et al. Embedding of Cortical Representations by the Superficial Patch System. Cereb Cortex. 2011;21(10):2244–2260.

48. Yoshimura Y, Callaway EM. Fine-scale specificity of cortical networks depends on inhibitory cell type and connectivity. Nature Neuroscience. 2005;8(11):1552–1559.

49. Cossell L, Iacaruso MF, Muir DR, Houlton R, Sader EN, Ko H, et al. Functional organization of excitatory synaptic strength in primary visual cortex. Nature. 2015;518:399–403.

50. Blakemore C, Tobin EA. Lateral inhibition between orientation detectors in the cat's visual cortex. Experimental Brain Research. 1972;15(4):439–440.

51. Nelson JI, Frost BJ. Orientation-selective inhibition from beyond the classic visual receptive field. Brain Research. 1978;139(2):359–365.

52. Bonds AB. Role of inhibition in the specification of orientation selectivity of cells in the cat striate cortex. Visual Neuroscience. 1989;2:41–55.

53. Nelson SB; San Diego California 92138. Robert Bosch Vision Research Center. Temporal interactions in the cat visual system. I. Orientation-selective suppression in the visual cortex. J Neurosci. 1991 2;11(2):344–56.

54. DeAngelis GC, Robson JG, Ohzawa L, Freeman RD. Organization of suppression in receptive fields of neurons in cat visual cortex. J Neurophysiol. 1992;68(1):144–163.

55. Walker GA, Ohzawa I, Freeman RD. Asymmetric Suppression Outside the Classical Receptive Field of the Visual Cortex. Journal of Neuroscience. 1999 12;19(23):10536–10553.

56. Freeman TCB, Durand S, Kiper DC, Carandini M. Suppression without inhibition in visual cortex. NEURON. 2002 8;35(4):759–771.

57. Shushruth S, Mangapathy P, Ichida JM, Bressloff PC, Schwabe L, Angelucci A. Strong recurrent networks compute the orientation tuning of surround modulation in the primate primary visual cortex. The Journal of neuroscience : the official journal of the Society for Neuroscience. 2012 Jan;32(1):308–21. Available from:

```
http://www.pubmedcentral.nih.gov/articlerender.fcgi?artid=3711470&
tool=pmcentrez&rendertype=abstract.
```

58. Hashemi-Nezhad M, Lyon DC. Orientation Tuning of the Suppressive Extraclassical Surround Depends on Intrinsic Organization of V1. Cerebral Cortex. 2012;22(2):308–326. Available from: `http://cercor.oxfordjournals.org/content/22/2/308.abstract`.

59. Sillito AM, Grieve KL, Jones HE, Cudeiro J, Davis J; London UK. Department of Visual Science. Visual cortical mechanisms detecting focal orientation discontinuities. Nature. 1995 11;378(6556):492–6.

60. Jin J, Wang Y, Swadlow HA, Alonso JM. Population receptive fields of ON and OFF thalamic inputs to an orientation column in visual cortex. Nat Neurosci. 2011 2;14(2):232–8.

61. Kisvárday ZF, Martin KAC, Freund TF, Maglóczky Z, Whitteridge D, Somogyi P. Synaptic targets of HRP-filled layer III pyramidal cells in the cat striate cortex. Experimental Brain Research. 1986;64:541–552.

62. Binzegger T, Douglas RJ, Martin K. A Quantitative Map of the Circuit of Cat Primary Visual Cortex. J Neurosci. 2004;24(39):8441–53.

63. Willmore BD, Mazer JA, Gallant JL. Sparse coding in striate and extrastriate visual cortex. Journal of neurophysiology. 2011;105(6):2907–2919.

64. McGuire BA, Gilbert CD, Rivlin PK, Wiesel TN. Targets of horizontal connections in macaque primary visual cortex. Journal of Comparative Neurology. 1991;305(3):370–392.

65. Kisvárday ZF, Eysel UT. Functional and structural topography of horizontal inhibitory connections in cat visual cortex. European Journal of Neuroscience. 1993;5(12):1558–1572.

66. Schwabe L, Obermayer K, Angelucci A, Bressloff PC. The Role of Feedback in Shaping the Extra-Classical Receptive Field of Cortical Neurons: A Recurrent Network Model. The Journal of Neuroscience. 2006 9;26(36):9117–9129.

67. Somogyi P, Kisvardy ZF, Martin KC, D W. Synaptic connections of morphologically identified and physiologically characterized large basket cells in striate cortex of cat. Neuroscience. 1983;10:261–294.

68. Adesnik H, Bruns W, Taniguchi H, Huang ZJ, Scanziani M. A neural circuit for spatial summation in visual cortex. Nature. 2012 10;490(7419):226–231.

69. Somers DC, Todorov EV, Siapas AG, Toth LJ, Kim DS, Sur M. A local circuit approach to understanding integration of long-range inputs in primary visual cortex. Cerebral Cortex. 1998;8(3):204–217. Available from: `http://cercor.oxfordjournals.org/content/8/3/204.abstract`.

70. Stetter M, Bartsch H, Obermayer K. A mean-field model for orientation tuning, contrast saturation, and contextual effects in the primary visual cortex. Biological cybernetics. 2000;82(4):291–304.

71. Rubin DB, Van Hooser SD, Miller KD. The Stabilized Supralinear Network: A Unifying Circuit Motif Underlying Multi-Input Integration in Sensory Cortex. Neuron. 2015;85(2):402–417.

72. Douglas RJ, Martin KAC. Neural Circuits of the Neocortex. Annual Review of Neuroscience. 2004;27:419–51.

73. Renart A, de la Rocha J, Bartho P, Hollender L, Parga N, Reyes A, et al. The Asynchronous State in Cortical Circuits. Science. 2010;327:587–590.

74. Dan Y, Atick JJ, Reid RC. Efficient coding of natural scenes in the lateral geniculate nucleus: experimental test of a computational theory. J Neurosci. 1996 5;16(10):3351–62.

75. Hartline HK. Inhibition of activity of visual receptors by illuminating nearby retinal areas in the Limulus eye. In: Federation Proceedings. vol. 8 (1); 1949. p. 69.

76. Kuffler SW. Discharge patterns and functional organization of mammalian retina. Journal of neurophysiology. 1953;16(1):37–68.

77. Singer W, Creutzfeldt OD; Max-Planck-Institute of Psychiatry. Reciprocal lateral inhibition of on- and off-center neurones in the lateral geniculate body of the cat. Experimental Brain Research. 1970;10(3):311–330.

78. Field DJ. Relations between the statistics of natural images and the response properties of cortical cells. JOSA A. 1987;4(12):2379–2394.

79. Litwin-Kumar A, Doiron B. Formation and maintenance of neuronal assemblies through synaptic plasticity. Nat Commun. 2014;5:5319.

80. Ko H, Cossell L, Baragli C, Antolik J, Clopath C, Hofer SB, et al. The emergence of functional microcircuits in visual cortex. Nature. 2013 4;496(7443):96–100.

81. Callaway EM, Katz LC. Emergence and refinement of clustered horizontal connections in cat striate cortex. Journal of Neuroscience. 1990 4;10(4):1134–1153.

82. Rozell CJ, Johnson DH, Baraniuk RG, Olshausen BA. Sparse coding via thresholding and local competition in neural circuits. Neural Computation. 2008;20(10):2526–2563.

83. King PD, Zylberberg J, DeWeese MR. Inhibitory interneurons decorrelate excitatory cells to drive sparse code formation in a spiking model of v1. The Journal of Neuroscience. 2013;33(13):5475–5485.

84. Furman M, Wang XJ. Similarity effect and optimal control of multiple-choice decision making. Neuron. 2008;60(6):1153–1168.

85. Beaulieu C, Colonnier M. The number of neurons in the different laminae of the binocular and monocular regions of area 17 of the cat. Journal of Comparative Neurology. 1983;217:337–344.

86. Kampa BM, Letzkus JJ, Stuart GJ; Mills Road ACT 0200 Canberra Australia. kampahifo.unizh.ch The John Curtin School of Medical Research. Cortical feed-forward networks for binding different streams of sensory information. Nat Neurosci. 2006 12;9(12):1472–3.

87. Perin R, Berger TK, Markram H. A synaptic organizing principle for cortical neuronal groups. Proceedings of the National Academy of Sciences. 2011 3;108(13):5419–5424.

88. Anderson JS, Carandini M, Ferster D. Orientation tuning of input conductance, excitation, and inhibition in cat primary visual cortex. Journal of neurophysiology. 2000;84(2):909–926.

89. Wong KF, Wang XJ. A recurrent network mechanism of time integration in perceptual decisions. The Journal of neuroscience. 2006;26(4):1314–1328.

90. Ahmed B, Anderson JC, Douglas RJ, Martin KA, Whitteridge D. Estimates of the net excitatory currents evoked by visual stimulation of identified neurons in cat visual cortex. Cerebral Cortex. 1998;8:462–476.

91. Nowak L, Azouz R, Sanchez-Vivez M, Gray C, McCormick D. Electrophysiological Classes of Cat Primary Visual Cortical Neurons In Vivo as Revealed by Quantitative Analyses. journal of neurophysiology. 2003;89:1541–1566.

92. Binzegger T, Douglas RJ, Martin K. Topology and dynamics of the canonical circuit of cat V1. Neural Networks. 2009;22(8):1071–1078.